JOINT INSTITUTE FOR NUCLEAR RESEARCH
Laboratory of Nuclear Problems

FINAL REPORT ON THE INTEREST PROGRAMME

Calculation of radiation shielding in a SPECT/CT scanner prototype using based on Monte Carlo code systems

Supervisor:
Dr. Antonio Leyva Fabelo

Student:
Daina Leyva Pernía, Cuba
Universidad de la Habana

Participation period:
8 February - 19 March, Wave 3

Dubna, 2021

Abstract

The objective of this work has been to familiarize with a SPECT/CT preclinical tomography facility, the biological protection shield integrated into it, and the calculation of the safe limit distance that guarantees the risk-free operation of this scanner for occupationally exposed personnel. Using the MCNPX code system for the simulation of radiation transport in materials, the dose rate distribution has been studied in a SPECT/CT scanner prototype. Two typical sources used in these devices were taken into consideration, as well as several geometric configurations, in order to determine for each the smallest distance to the center of the equipment that can be considered safe for occupationally exposed personnel. As reference for comparisons, the values reported by the International Commission on Radiological Protection were used. The results showed that for the selected geometric conditions for the SPECT method, using a 99mTc source, and in the absence of the gantry and the lead shielded wall, the accepted distance limit in X and Y axis are in the intervals between 15.03 - 19.14 cm, and 22.98 - 23.35 cm respectively. Under these same geometric conditions, but using as a source the X-rays of a W tube, it is obtained that the safe limit distances on the X axis are: 566 cm on the left (in the opposite direction to the source emission vector), and 6757 cm on the right, while on the Y axis, the results obtained are almost symmetric with respect to the center of coordinates: 1449 cm above and 1421 cm below. When two walls are introduced around the target-source-detector arrangement, one of duralumin simulating the gantry, and the other of lead shielding, both of 1 cm, these results are significantly modified. These additions cause the safe distances obtained for the simplest CT setup to decrease by 50.7% in the region to the left and by 95.9% to the right of the coordinate center, while in the Y axis the decrease, both above and below, is 74%. More details on these results and their analysis are presented in the text.

Introduction

Any device that in its operation uses some source of ionizing radiation, must necessarily guarantee its safety for the health of occupationally exposed personnel.
That is why during its development, and before putting it into operation, it requires a large number of tests and trials to ensure that when used they are as harmless as possible to man. Especially important are those diagnostic and medical treatment techniques that use ionizing radiation, as the common X-ray equipments, the sophisticated gamma cameras or PET and SPECT scanners.
In these studies, the mathematical modeling of radiation transport plays an important role; see for example [1, 2].
In this Report, with the use of mathematical simulation we are going to calculate the distribution with the distance of the dose rate for different geometries and sources in the vicinity of a preclinical SPECT/CT hybrid scanner system (in figure 1 illustrative image).
The main objective is to determine the working distance considered safe for the occupationally exposed personnel. The based-on Monte Carlo method code system MCNPX was used for this.

Figure 1. Illustrative image. Commercial hybrid SPECT/CT scanner system.

Materials and Methods

SPECT/CT tomography

The computed tomography (CT) is a computerized X-ray imaging procedure in which a narrow beam of X-rays is aimed at a patient and quickly rotated around the body, producing signals that are processed by computer to generate cross-sectional images of the body [3]. These “slices” are collected and they can be digitally “stacked” together to form a three-dimensional image of the patient that allows for easier identification and location of basic structures as well as any possible abnormalities.

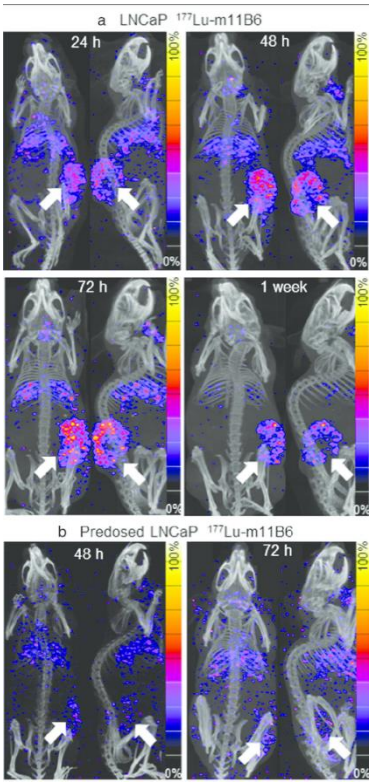

Figure 2. Illustrative image. SPECT/CT imaging of a mouse.

The combination of CT with other techniques has produced a new generation of equipment known as hybrid scanners, a new paradigm in obtaining medical and scientific images able to merge the obtained anatomical information with the functional.

Among these hybrid techniques, SPECT/CT stands out, combining SPECT tomography ("Single Photon Emission Computed Tomography") and computed tomography into one imaging system. Figure 2 presents, as an example, a set of images obtained in a preclinical SPECT / CT scanner to assess the quality and variety of the information obtained [4].

SPECT tomography is a 3D nuclear medicine tomographic imaging technique using gamma rays [5]. The technique requires delivery of a gamma-emitting radioisotope into the patient, usually through injection into the bloodstream. Generally, radioisotope is attached to a specific ligand to create a radioligand, whose properties bind it to certain types of tissues. This conjugal allows the combination of ligand and radiopharmaceutical to be carried and bound to a place of interest in the body, where the ligand concentration is seen by a gamma camera.

The SPCT/CT combination has many advantages that are reported in the literature, for example in [6, 7].

Sources

A preclinical SPECT/CT scanner, as explained above, uses two types of radioactive sources. The first is the X-ray tube from the CT procedure, and the second is the gamma radioisotopic source injected into the animal under study.

For the simulation of the CT configuration, the W anode X-ray tube was approximated to a point source positioned 1 mm in front of the anode. This source emits only in the phantom direction within a solid angle 20^{o}. The full X-ray tube energy spectrum was considered in the simulation and it was calculated using interpolating polynomials (TASMIP) for 120 keV (figure 3) [8].

In the case of SPECT configuration, among the radioisotopes commonly used in this technique (^{57}Co, ^{68}Ge, ^{99m}Tc, ^{111}In, ^{123}I, etc.), ^{99m}Tc (140 keV) was selected (in figure 4, the decay scheme of ^{99}Mo and ^{99m}Tc). The source was positioned in the center of mouse phantom, inside of a sphere simulating the heart, emitting homogeneously in all directions. The activity of the source is 10 MBq.

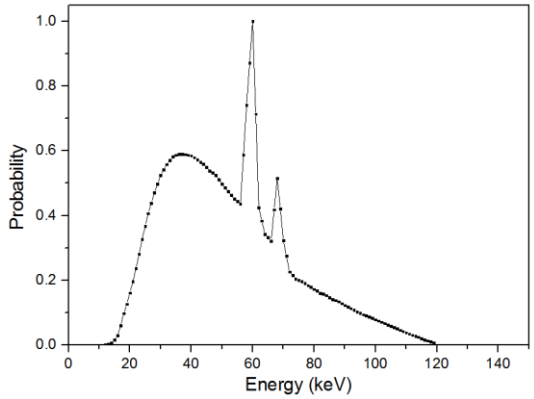

Figure 3. The tungsten anode spectrum.

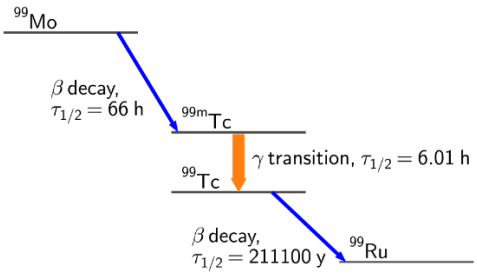

Figure 4. Decay scheme of ^{99}Mo and ^{99m}Tc.

MCNPX

The MCNPX ("Monte Carlo N - Particle") [9], is a 3D code consisting of a group of subroutines for sequential simulation by the Monte Carlo Method [10] of the individual probabilistic events that make up the transport processes of 34 types of different particles and photons, in a geometric configuration given three-dimensional and with a varied composition of materials. It is fundamentally based on the use of the effective section of each type of interaction and the statistical nature of the transport process to predict the probability of distribution of specific parameters such as energy losses and angular detection.
During the simulation of the interactions, the program will take into account all the specifications entered by the user in the input file. This file contains the information about the materials that will be involved in the interaction process, the geometry of the experiment, the characteristics of the source and the outputs desired by the user (Tally). All the outputs used from the MCNPX are normalized by the number of incident particles from the source (or the number of stories calculated) and are reported together with their estimated relative error.
In presented here simulations we use the tally F5 for obtaining the particle fluency at selected positions, the cards DE, DF and FM to convert the F5 results to dose rate units, and 10^8 histories for obtaining a good statistic.

Dose treatment

For professionals, - persons who are exposed to radiation from technical sources and are under dose surveillance, e.g. medical personnel or workers in a nuclear installation wearing a personal dosimeter - a whole-body dose rate of 20 mSv/year is permitted, which means that about 2.3 μSv/hour considered safe [11, 12]. See Table 1. For the conversion of the outputs obtained by the code system from flow units to dose units, were used the coefficients recommended by [13]. This conversion is done using the DE and DF cards of the MCNPX.

Table 1. Dose limits a year for different human groups.

	Employees &Trainees (18+y)	**Trainees** under 18y	**Other persons**
Whole body – effective dose	**20mSv**	**6mSv**	**1mSv**
Lens of Eye	20mSv	15mSv	15mSv
Skin	500mSv	150mSv	50mSv
Hands, forearms, feet & ankles	500mSv	150mSv	50mSv

Results

The calculations were performed independently for each of the two techniques contemplated in SPECT/CT. Next, the results obtained independently for each of them will be presented, in parallel they will be analyzed, and where appropriate, partial conclusions will be given.

SPECT

The figure 5 shows the geometric arrangement used for the determination of the dependence of the dose rate with the distance from the source by means of the mathematical modeling. The photon source (^{99m}Tc) is positioned just in the coordinate center (0, 0, 0). The figure identifies the different components, so we will not describe them. Intentionally, the gantry and any other radiological protection, were not considered.

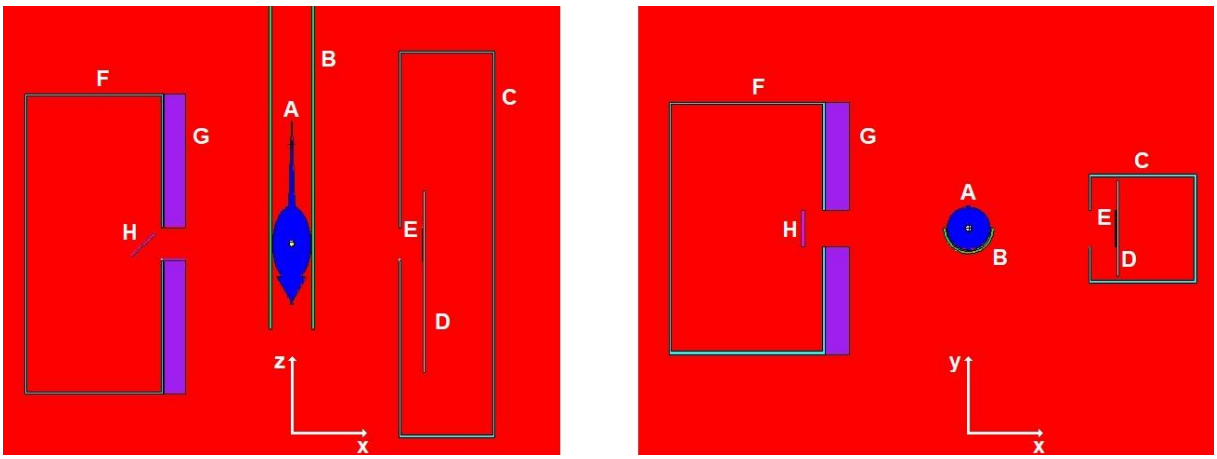

(a) (b)

Figure 5. Schematic representation of the geometric arrangement considered in the calculations; (a) - view in the xz plane, and (b) - view in the xy plane. A - mouse, B - polypropylene bed, C - stainless 202 protective case for detector, D - Fiberglass detector support, Type C (PCB), E – 500 µm GaAs:Cr detector, F - stainless 202 protective case for X-ray tube, G - duralumin protective plate, H - W anode of X-ray tube.

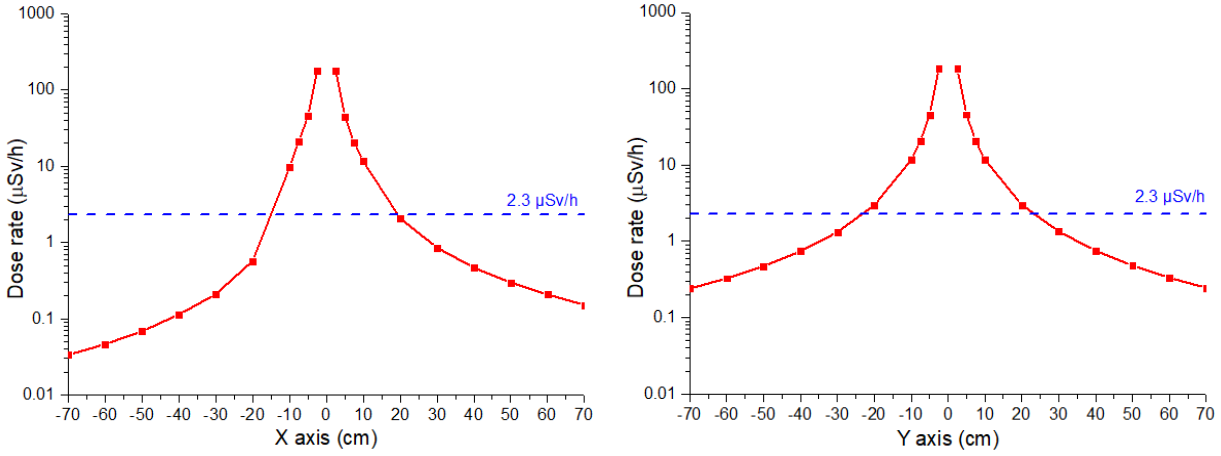

(a) (b)

Figure 6. Dose behaviors with the distance in X (a) and Y (b) axes.

To compare the calculated doses and the considered reference safe values, the figures 6 (a) and (b) are presented. They show the dose behaviors with the distance in X and Y axes.
Along the X axis, it was obtained that to the left of the mouse (in the center of which the source is placed) the accepted dose rate limit is reached at **-15.03 cm**, while to the right the limit is **19.14 cm**. In this axis there are obstacles where a substantial absorption of radiation occurs: the steel protection boxes of the X-ray source and detector, the detector itself with its support or printed circuit, and the anode of the X-ray tube.
In the Y axis the dose rate limit value for occupationally exposed workers is reached at **-22.98 cm** below the position of the source, and at **23.35 cm** above it. The difference is motivated exclusively by the presence of the polypropylene bed on which the mouse is positioned.
These values are small compared to the dimensions of the installation, so it should not be a concern for specialists who handle the scanner. Furthermore, the scanner must also have a series of parts, such as the gantry, which is a powerful screen for radiation, and also a biological protection, generally made of lead, which reliably protects against any unnecessary and dangerous exposure. We will include these add-ons in the next analysis for the CT part of the scanner.

CT

For CT, the simulation was carried out on the same experimental arrangement as for SPECT, except that instead of the point source placed inside the mouse, an X-ray source with W anode was used, as explained above, positioned in the coordinates (-13.6, 0, 0), which is quite close to a real distance on some real scanners.
The distribution of the calculated dose rate with the distance for this case is shown in figures 7 (a) and (b) on the X and Y coordinate axes, respectively.

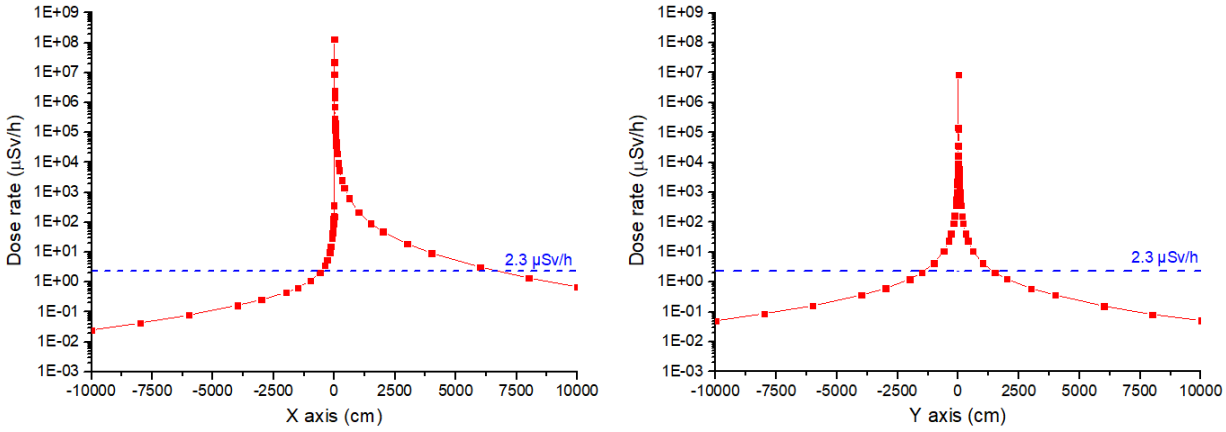

(a) (b)

Figure 7. Dose rate behaviors with the distance in X (a) and Y (b) axes and Z = 0.

Figures 7 (a) and (b) show the results of the performed calculations on the X and Y axes, observing that the distances were the limit values are considered safe (2.3 µSv/h) now have increased appreciably comparing with the previous example. In this configuration the safe limits on the X axis are: **566 cm** on the left (in the opposite direction to the source emission vector), and **6757 cm** on the right. For the Y axis, the results obtained are almost symmetric with respect to the center of coordinates: **1449 cm** above and **1421 cm** below. The very high values of safe distance, compared to those obtained in the SPECT technique, are the result of the characteristics of the sources. The X-ray tube emits a flux

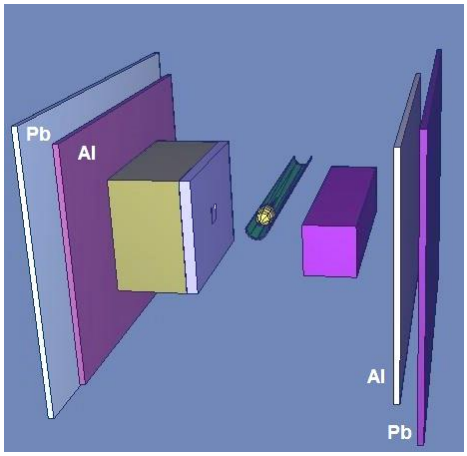

Figure 8. 3D view of the simulation geometry with the introduction of the Al and Pb walls.

of photons oriented towards the target in a small angle, resulting in our case 6 orders higher than that emitted by the isotopic point source used.

Taking these results into account, it is convenient to introduce two additional protection walls on the X axis. The first wall would correspond in the real equipment with the wall of the duralumin gantry, and the second one is the external protection of the system, made with Pb. Both walls have a thickness of 1 cm. Figure 8 shows the scheme of the geometric arrangement, only identifying the aggregate walls; everything else is identical to figure 5.

The results of the calculation are presented in figures 9 (a) and (b). As it is shown, the effect of the added walls is significant. On the X axis, safe distances have now shifted to **285 cm** on the left (represents **49.7%** decrease) and **280 cm** on the right (represents **95.9%** decrease) with respect to the coordinate center. In the Y axis, the addition of the gantry and 1 cm Pb wall in X axis, leads to the fact that the safe distance limits are now shifted to **1357 cm** on the positive side of the axis and **1342 cm** on the negative side, which constitutes a decrease of **5.6%** and **6.4%** respectively.

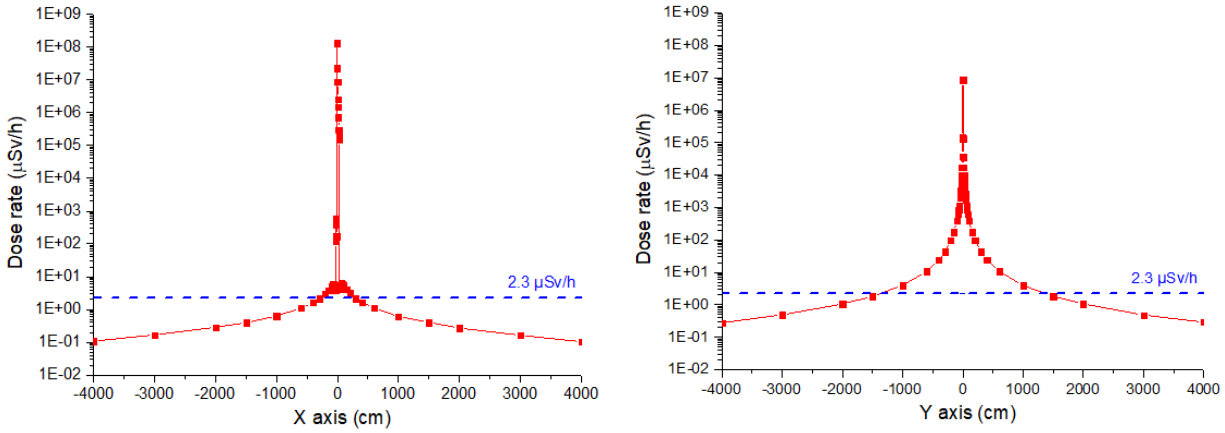

(a) (b)

Figure 9. Dose rate behaviors with the distance in X (a) and Y (b) axes and Z = 0 for the geometry where protection walls were inserted in X axis.

Figure 9 (a) seems to indicate that the asymmetrical shape of dependency found in figure 7 (a) has been lost, but that is only a visual effect produced by the marked difference in scales. To verify it, figure 10 is presented, where figure 9 (a) was taken and the scale near the center of coordinates has been extended. For a better general understanding, the parts of the geometry that most strongly affect the transport of photons are shown in the image.

Observing the high dose rate values obtained on the Y axis, it is advisable to place a protection on that axis that attenuates the flow of photons to reduce the safe limit distance. Adding on the Y axis (and perpendicular to it) two walls such as those placed in X, of the same materials, thicknesses and located at the same distances from the center, then the simulation of the dependence of the dose rate as a function of the distance shows the results presented in figures 11 (a) and (b).

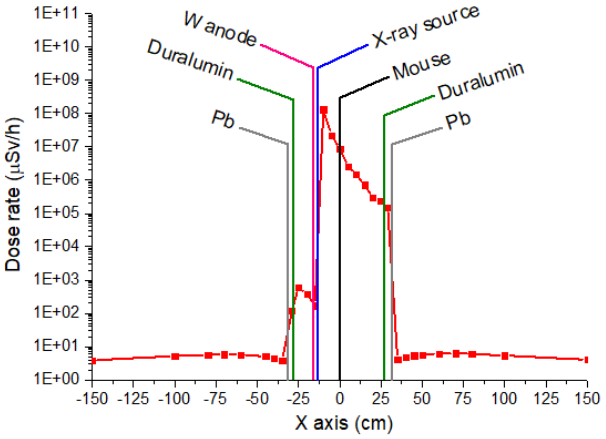

Figure 10. Details of the central region of figure 9 (a) on an extended scale, where the positions of the most important features are indicated.

Now that the shield is arranged in the two coordinate axes, it is obtained that in the X axis with respect to the values obtained from figure 7 (a), the safe limit distance decreases to the left in **50.7%** and **95.9%** at the right. In other words, in this axis the additional contribution to security is minimal. However, on the Y axis this decrease is substantial and constitutes **74%**. As a result, in this configuration the safe limit distances for the protection of occupationally exposed personnel that were obtained are: **278 cm** in front and behind the source, and **375 cm** above and **370 cm** below it (always with respect to the center of coordinates).

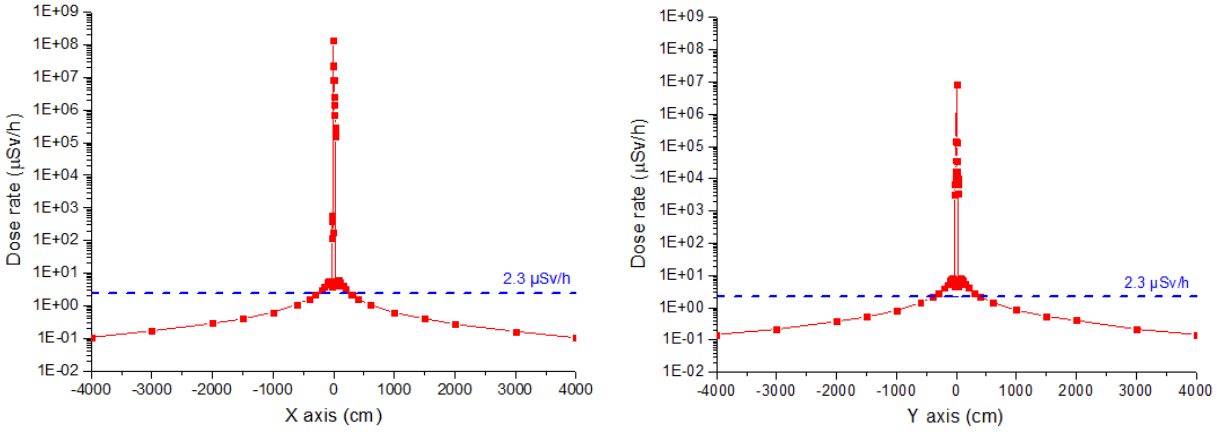

(a) (b)

Figure 11. Dose rate behaviors with distance in X (a) and Y (b) axes and Z = 0, for the geometry where additional protection walls were inserted also in Y axis.

It is worth mentioning that the inclusion of a duralumin wall is simply an approximation of an important part of scanners of this type, which is the gantry. The gantry is made of aluminum or steel, or their alloys, and its main function is to support sources and detectors and allow them to sweep around the target under study. Obviously, as the gantry surrounds the sources and detectors, it constitutes a shielding for the radiation exit path. The lead wall is the protection par excellence of these scanners and its thickness and geometry is selected depending on the energy, activity of the sources, shape and dimensions of the tomograph, etc. In practice, within a scanner there are many more pieces made of metal and other materials that are intentionally placed to attenuate radiation and protect people and systems, such as associated electronics. But there are also many more details, which without being intended for that, contribute to the protection against radiation.

Conclusion

Using the MCNPX code system for the simulation of radiation transport in materials, the dose rate distribution has been studied in a SPECT/CT scanner prototype. Two typical sources used in these devices were taken into consideration, as well as several geometric configurations, in order to determine for each, the smallest distance to the center of the equipment that can be considered safe for occupationally exposed personnel. The results showed that for the selected geometric conditions of the SPECT method, using a ^{99m}Tc source, and in the absence of the gantry and the lead shielded wall, the accepted limit distance in X axis is 15.03 cm to the left of the center of coordinates, and 19.14 cm to the right, while on the Y axis these limits are 22.98 cm above and 23.35 cm below the center. Under these same geometric conditions, but using the X-rays of a W tube as a source, it is obtained that the safe limit distances on the X axis are: 566 cm on the left (in the opposite direction to the source emission vector), and 6757 cm on the right, while on the Y axis, the results obtained are almost symmetric with respect to the center of coordinates: 1449 cm above and 1421 cm below. When two walls are introduced around the target-source-detector arrangement, one of duralumin simulating the gantry, and the other of lead shielding, both of 2 cm, these results are significantly modified. These additions cause the safe distance obtained for the simplest CT setup to drop by 50.7% in the region on the left, and by 95.9% on the right. In the Y axis the decrease, both above and below it is 74%. More details on these results and their analysis are presented in the text.

References

1. M. Z. Abdul Aziz, S. Yani, F. Haryanto, et al., Monte Carlo simulation of X-ray room shielding in diagnostic radiology using PHITS code, Journal of Radiation Research and Applied Sciences **13**(1), 704, (2020).
2. L. Tourinho, F. Machado de Jesus, E. Alves de Souza, et al., Computed tomography x-ray characterization: A Monte Carlo study, Radiation Physics and Chemistry **167**, 108359, (2020).
3. J. Hsieh, Computed Tomography: Principles, Design, Artifacts, and Recent Advances, Third Edition, PM259, (2015).
4. O. Timmermand, E. Larsson, D. Ulmert, et al., Radioimmunotherapy of prostate cancer targeting human kallikrein-related peptidase 2, EJNMMI Research **6**(1), 27, (2016).
5. Wernik M. N. and Aarsvold J. N., Emission Tomography: The Fundamentals of PET and SPECT, Elsevier Academic Press, (2004).
6. Perera A., Torres L. A., Vergara A., et al., SPECT/CT: main applications in nuclear medicine, Nucleus, 62, (2017).
7. Bural G. G., Muthukrishnan A., Oborski M. J., et al., Improved Benefit of SPECT/CT Compared to SPECT Alone for the Accurate Localization of Endocrine and Neuroendocrine Tumors, Mol. Imaging Radionucl Ther. 21(3), 91, (2012).
8. J. M. Boone and J. A. Seibert, An accurate method for computer-generating tungsten anode X-ray spectra from 30 to 140 kV, Med Phys. 24(11), 1661, (1997).
9. Hendricks J. S., LA-UR-08-2216, "MCNPX 2.6.0 Extensions", Los Alamos National Laboratory, April 11, (2008).
10. Rubinstein R. Y. and Kroese D. P., Simulation and the Monte Carlo Method, Third ed., John Wiley & Sons Inc., (2017).
11. The Ionising Radiations Regulations 2017 (IRR17), Guidance - Part 2 - General Principles and Procedures, UK Statutory Instruments, No. 1075, (2017).

12. International Commission on Radiological Protection, ICRP-103 The 2007 Recommendations of the International Commission on Radiological Protection, JAICRP 37, (2007).
13. ICRP, Conversion Coefficients for Radiological Protection Quantities for External Radiation Exposures. ICRP Publication 116, Ann. ICRP 40(2–5), 125, (2010).

Acknowledgments

I would like to thank my supervisor, Dr. Antonio Leyva Fabelo, for all the help, guidance and support offered during the projecy. I would also like to acknowledge JINR for the wonderful opportunity of participating in this interesting project. This has been a very educational activity for me, and the knowledge and abilities I have acquired during it are going to be extremely useful in my future in science.